RSC Advances

PAPER

View Article Online
View Journal | View Issue

Cite this: *RSC Adv.*, 2026, **16**, 25999

New fused tetracyclic ring systems: synthesis of 1-thia-4*a*,11,12-triazatetracenes *via* a multicomponent strategy, 2D-HMBC structural confirmation, and antimicrobial activity

Reham E. Abdelwahab, [a] Mostafa E. Salem, [b] Mohammed Rashed Alsulami,[a] Mona M. Soliman, [c] Ismail A. Abdelhamid, *[a] Amr Mohamed Abdelmoniem, [a] Faisal K. Algethami [b] and Ahmed H. M. Elwahy *[a]

We report a novel synthetic strategy for tetracyclic heterocycles, specifically 1-thia-4*a*,11,12-triazatetracenes, representing a previously unreported fused ring system, using enamine 8-amino-3,4-dihydropyrimido[2,1-*b*][1,3]thiazin-6-one as a versatile building block. This enamine undergoes multicomponent reactions with aldehydes and dimedone in refluxing acetic acid, efficiently affording the target fused heterocycles. Structural elucidation was confirmed *via* alternative synthetic routes and 2D-HMBC correlations. The resulting compounds possess a rigid, planar, and highly conjugated tetracyclic framework enriched with heteroatoms (N, S, O), features known to enhance binding interactions with biological macromolecules. Such structural characteristics favor interactions within enzyme active sites, particularly nucleic acid–processing enzymes such as DNA-directed RNA polymerase, as a putative target based on molecular docking predictions. Among the synthesized series, compound **9a** emerged as a potent broad-spectrum agent, demonstrating strong antibacterial activity against all tested strains, with notable efficacy against *S. aureus* (MIC = 0.5 mg mL^{-1}). Molecular docking studies corroborated its bioactivity, predicting higher binding affinity of **9a** against *Aspergillus terreus* (ΔG = −9.2 kcal mol^{-1}) compared to fluconazole, and stronger predicted affinity against the bacterial target than tetracycline (ΔG = −6.7 kcal mol^{-1}). These results position **9a** as a promising lead for further antimicrobial development.

Received 9th April 2026
Accepted 8th May 2026

DOI: 10.1039/d6ra03008d

rsc.li/rsc-advances

Introduction

Enamines are extremely accessible reagents, and the nucleophilic nature of C-2 has been utilized in various synthetic organic chemistry applications.[1–4] Multicomponent reactions (MCRs) are an intriguing synthetic method because they enable selectivity, atom economy, simplicity, and rapid access to synthetic organic molecules.[5–11] The Hantzsch reaction is a popular multicomponent route for synthesizing 1,4-dihydropyridines. These compounds have many biological and pharmacological uses, such as anticancer,[12] antiviral,[13] anti-inflammatory,[14] anti-Alzheimer activity,[15] and anticonvulsant.[16] Over the past few years, organic and medical scientists have also been interested in heterocycles that contain nitrogen as well. Among them, pyridines[17–21] and pyrimidines[22–25] are also biologically essential heterocycles that exhibit considerable biological characteristics. Quinolines were also discovered to exhibit a broad spectrum of biological activities, such as antimalarial, antibacterial, antihypertensive, anticancer, anti-asthmatic, and antituberculosis qualities.[26–31] Additionally, it has been shown that pyrimidoquinolines have strong biological properties, including anti-inflammatory,[32,33] anti-cancer,[34–37] antibacterial,[32,38,39] antioxidant,[32] antimalarial,[27] and analgesic[39,40] effects. Additionally, the idea of hybrid pharmaceuticals introduced a new approach to drug design that combines two or more drugs with inherent activity into a single agent in order to address the issue of drug resistance.[41,42] The majority of these hybrids reduce the likelihood of drug resistance since the two pharmacological medications have separate mechanisms of action against distinct targets. Molecular hybridization is regarded as a potent technique for creating molecules with multiple structural units that have better bioactivities than their lead counterparts.[43] Recently, we reported how to create bis(aminothiouracil) **3** by reacting 1,3-dibromopropane **2** with two mole equivalents of 6-aminothiouracil **1**. Next, we investigated the utility of bis(aminothiouracil) **3** in the synthesis of some novel bis(tetrahydropyrimido[4,5-*b*]quinoline-4,6-dione) **4**, which are connected by a bis(sulfanediyl) linker (Fig. 1).

[a]*Department of Chemistry, Faculty of Science, Cairo University, P. O. 12613, Giza, A. R. Egypt. E-mail: ismail_shafy@cu.edu.eg; aelwhy@cu.edu.eg*

[b]*Chemistry Department, College of Science, Imam Mohammad Ibn Saud Islamic University (IMSIU), P. O. Box 90905, Riyadh 11623, Saudi Arabia*

[c]*Department of Botany and Microbiology, Faculty of Science, Cairo University, Giza 12613, Egypt*

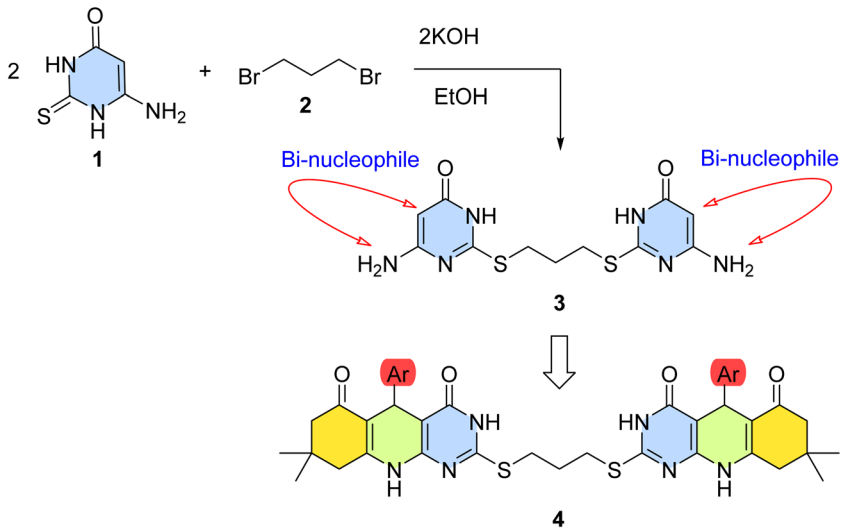

Fig. 1 Previously reported synthesis of bis(aminothiouracil) derivatives and their conversion into bis(tetrahydropyrimido[4,5-*b*]quinoline-4,6-dione) structures.

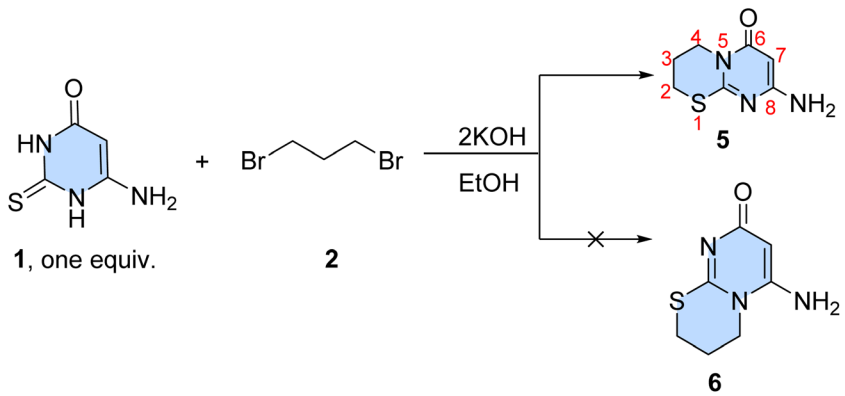

Scheme 1 *S*-alkylation of 6-aminothiouracil (**1**) with 1,3-dibromopropane (**2**) in the presence of anhydrous KOH.

Results and discussion

As part of our continuing interest in the synthesis of heterocycles,[44–67] in the current study, we extend our investigation utilizing 8-amino-3,4-dihydropyrimido[2,1-*b*][1,3]thiazin-6-one **5** as the building block for our target molecules. Compound **5** was synthesized through an *S*-alkylation reaction of 6-aminothiouracil (**1**) with one equivalent of 1,3-dibromopropane (**2**), employing two equivalents of anhydrous KOH as the base (Scheme 1). Theoretical simulations and nuclear magnetic resonance spectroscopy ruled out the other potential isomer, 6-amino-3,4-dihydropyrimido[2,1-*b*][1,3]thiazin-8-one **6**.[68,69]

Compound **5** is regarded as an enamine, and C7 is more nucleophilic than the NH_2 group due to the delocalization of the amino group's lone pair of electrons (Fig. 2). Consequently, it reacts with benzaldehyde **8a** and dimedone 7 to produce the addition product, which may be expressed as either 7-phenylhexahydro[1,3]thiazino[3′,2′:1,2]pyrimido[4,5-*b*]quinoline-6,8-dione **9a** or its regioisomeric, 5-phenylhexahydro[1,3]thiazino[3′,2′:1,2]pyrimido[4,5-*c*]isoquinoline-4,13-dione **10a** (Scheme 2).

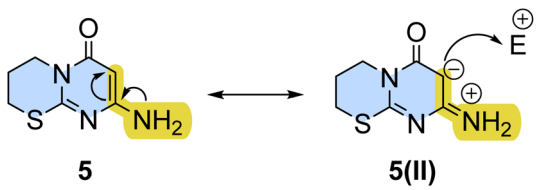

Fig. 2 Representation of compound **5** as an enamine, highlighting the nucleophilic character of C7 due to delocalization of the amino group's lone pair of electrons.

Despite the inability of the ^{1}H-NMR and ^{13}C-NMR spectra to clearly distinguish between isomers **9a** and **10a**, the HMBC spectrum of the isolated molecule suggests that **9a** was formed as the sole product. Accordingly, the best evidence for our suggested structure is the ^3J-coupling cross-correlations between the H7 signal at $\delta = 4.88$ ppm and the two carbonyl

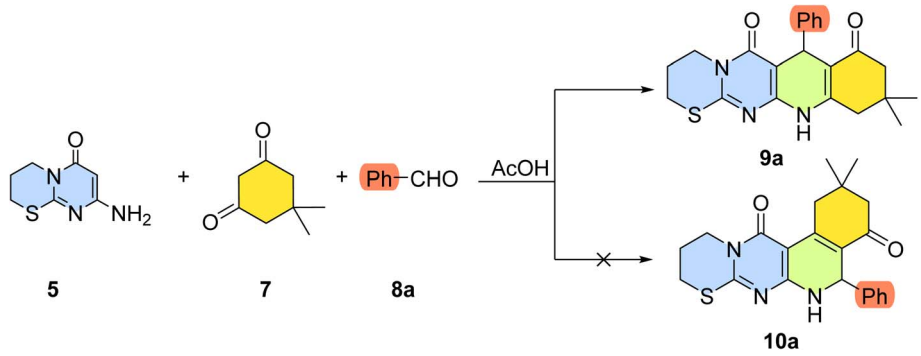

Scheme 2 Reaction of enamine (**5**) with benzaldehyde (**8a**) and dimedone (**7**) under acidic conditions.

groups in compound **9a**, δ = 160.6 and 194.3 ppm (Fig. 3). Otherwise, just one carbonyl and H-5 would have displayed ^{3}J-CH cross-correlations in isomer **10a**.

Scheme 3 shows a plausible reaction pathway for **9** and **10**. Initially, acetic acid, serving as an acidic catalyst, enhances the electrophilicity and reactivity of the carbonyl group in aldehydes **8** towards dimedone **7** *via* a Knoevenagel condensation reaction, resulting in the formation of the required 2-arylidene intermediate **11**. There are two possible paths for the Michael addition of C–H7 and NH_2 of 8-amino-3,4-dihydropyrimido[2,1-*b*][1,3]thiazin-6-one towards Michael-acceptor **11** (paths A and B). The first nucleophilic interaction of compound **5**'s H7 to the activated β-carbon of arylidene-dimedone **11** forms compound **12**. Michael adducts **13** are produced through cyclization, which involves the nucleophilic addition of compound **12**'s NH to the activated carbonyl. Compound **9** is formed through the intermediacy of **14** by removing a water molecule. Route B involves adding the amino group of compounds **5** to the β-carbon of arylidene-dimedone **11**, accompanied by nucleophilic addition of C–H7 to the activated carbonyl of compound **15** to create

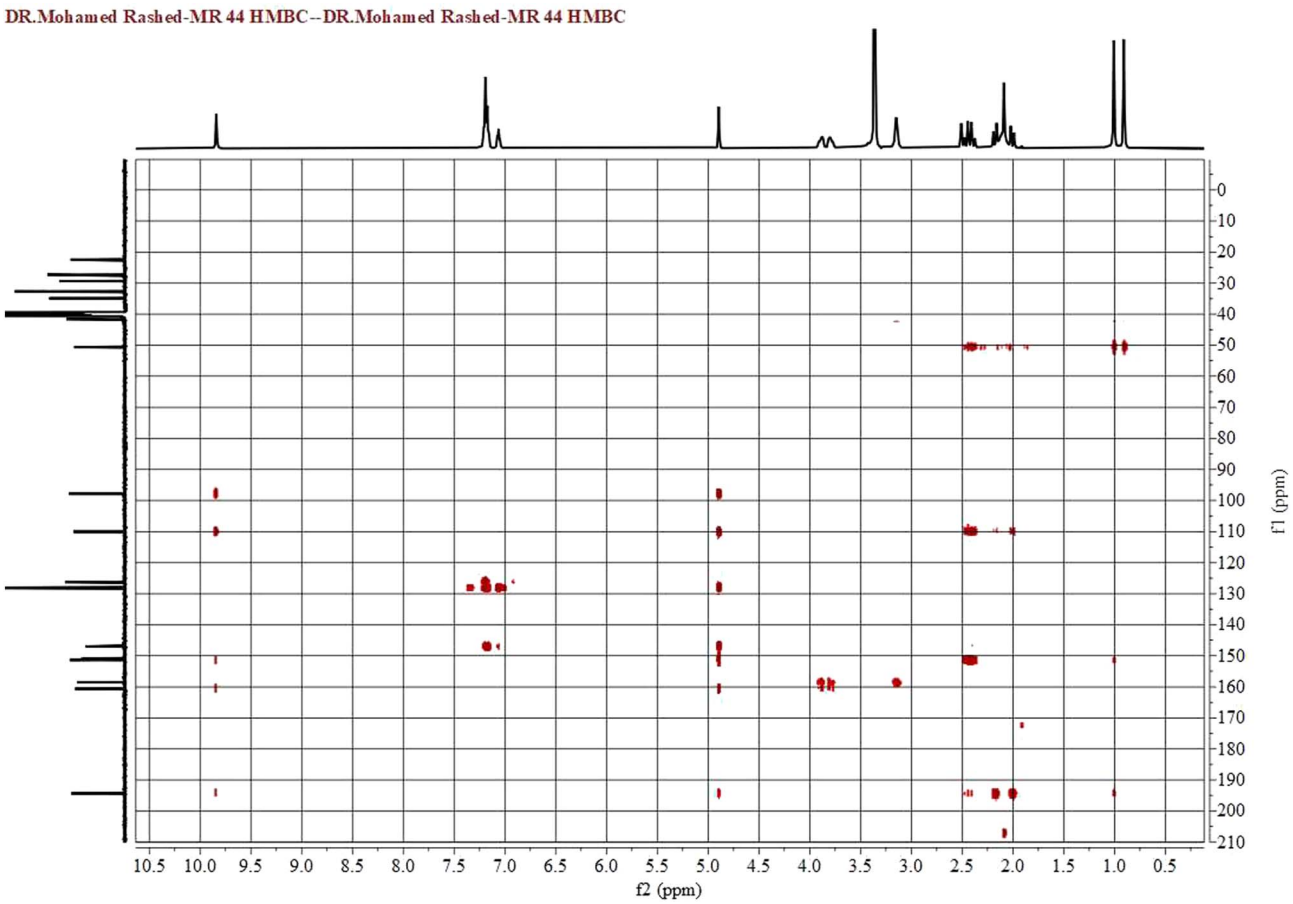

Fig. 3 HMBC correlations confirming the structure of compound **9a**.

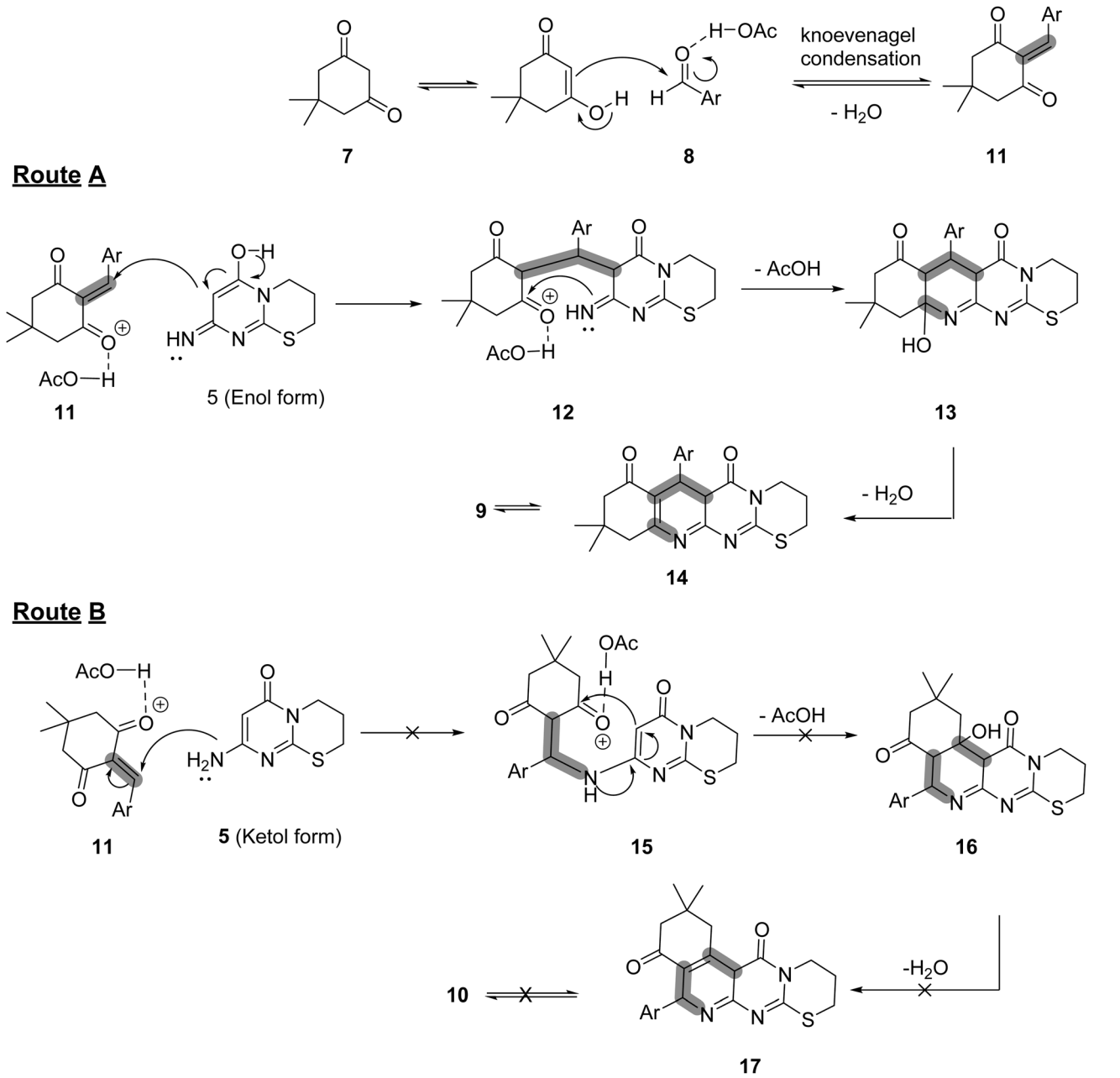

Scheme 3 Proposed reaction mechanism for the formation of tetracyclic heterocycles **9** and **10**.

Michael adduct **16.** Compound **10** is formed *via* intermediacy of **17** after acid catalyst and water removal.

It is noteworthy that *S*-alkylation of 5-phenyl-2-thioxohexahydropyrimido[4,5-*b*]quinoline-4,6-diones **18a** with one equivalent of 1,3-dibromopropane **2** in the presence of two equivalents of KOH led to the formation of the same product **9a**, thus confirming the proposed structural assignment. Compound **18a**[70] was independently synthesized by refluxing **1**, benzaldehyde **8a**, and dimedone **7** in acetic acid, as shown in Scheme 4 (procedure B).

Inspired by this accomplishment, we expanded the reaction's scope to create 7-arylhexahydro[1,3]thiazino[3′,2′:1,2]pyrimido[4,5-*b*]quinoline-6,8-dione, which is connected to different aryl moieties at position-7 through the utilization of diverse aldehydes. Accordingly, the Hantzsch products **9b–g** are produced in good yields when one equivalent of compound **5** reacts with one equivalent of the aldehydes **8b–g** and dimedone **7** (Scheme 5, method A). Similarly to compounds **9a**, compounds **9b–g** were alternatively produced *via* the alkylation of the initially obtained 5-aryl-2-thioxohexahydropyrimido[4,5-*b*]quinoline-4,6-diones **18b–g**[70] with the 1,3-dibromopropane **2** in a basic medium (Scheme 5, method B).

In both cases, the reported yields correspond to the overall yields for the formation of compound **9** starting from the same precursors. In method A, the sequence involves initial alkylation followed by the three-component cyclocondensation,

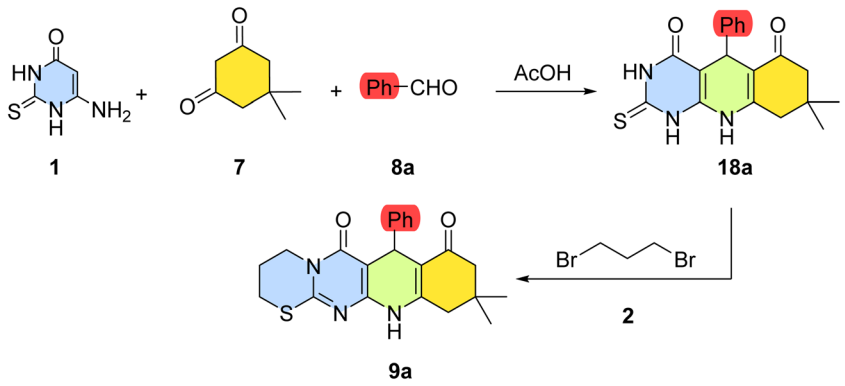

Scheme 4 Alternative synthetic route for compound **9a**.

whereas in method B, the three-component reaction is performed first to afford intermediate **18**, followed by a subsequent alkylation step to give **9**. The comparison is therefore intended to highlight the effect of reaction sequence on the overall efficiency of the synthetic route (Table 1).

We also explored *ortho*-substituted benzaldehydes; however, repeated attempts did not afford isolable pure products, likely due to steric hindrance affecting the key condensation step and/or subsequent cyclization. This observation is consistent with the increased steric demand at the *ortho* position.

The synthesized compounds are fused tetracyclic heterocycles (1,2,3*a*,10,11-pentaza-5*H*-cyclopenta[*b*]anthracene-4,6-diones) with acene-like topology but reduced aromaticity due to heteroatom incorporation and partial saturation (Fig. 4). It has been reported that heteroatom substitution within acene-like structures changes their biological activity.[71–74]

Antimicrobial activity

The antimicrobial screening of seven synthetic compounds against two Gram-positive bacteria (*Staphylococcus aureus*, *Enterococcus faecalis*), one Gram-negative bacterium (*Escherichia coli*), and one fungus (*Aspergillus terreus*) revealed a distinct spectrum of activity, as shown in Table 2 and Fig. 5. Compound **9a** demonstrated the broadest spectrum, exhibiting activity against all four tested microorganisms. In terms of potency, the largest inhibition zones were recorded for compound **9a** against *S. aureus* (9.67 ± 1.53 mm), followed by compound **9f**, which shows high activity against *E. coli* (8.67 ± 0.58), which may be due to the presence of three methoxy groups. Mohamed *et al.* (2012) suggested that chalcone derivatives containing electron-releasing groups, such as OCH_3, increase antimicrobial activity. The antimicrobial activity of compounds may be due to damage

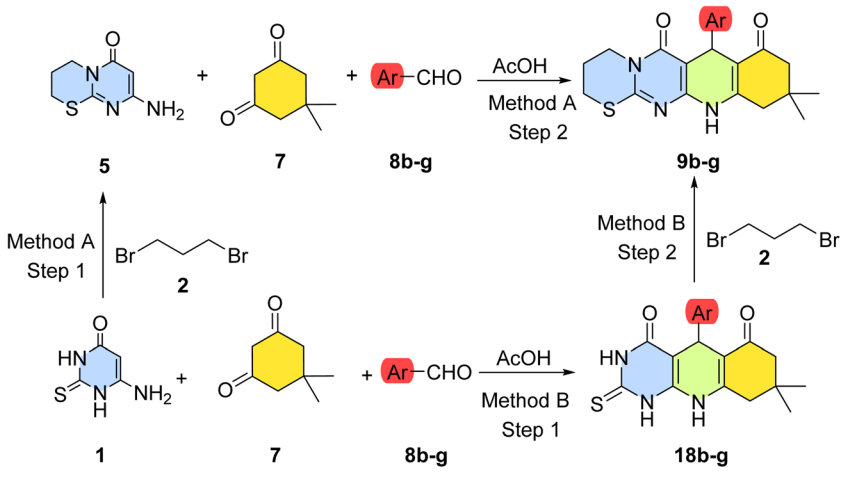

8,9,18b, Ar = 4-ClC_6H_4
8,9,18c, Ar =4-MeC_6H_4
8,9,18d, Ar =4-$MeOC_6H_4$
8,9,18e, Ar =4-$NO_2C_6H_4$
8,9,18f,Ar =3.4,5-$(MeO)_3C_6H_2$
8,9,18g, Ar =

Scheme 5 Synthesis of 7-arylhexahydro[1,3]thiazino[3′,2′:1,2]pyrimido[4,5-*b*]quinoline-6,8-diones (**9b–g**) using the two methods A and B.

Table 1 Overall yields (%) for the synthesis of compounds **9a–g** *via* two-stepwise sequences: method A (alkylation followed by cyclo-condensation) and method B (cyclocondensation followed by alkylation)

Entry	Ar[1]	Overall yield (%)	
		Method (A)	Method (B)
9a	C_6H_5–	77	69
9b	4-ClC_6H_4–	87	84
9c	4-MeC_6H_4–	82	75
9d	4-$MeOC_6H_4$–	87	79
9e	4-$O_2NC_6H_4$–	85	81
9f	3,4,5-$(MeO)_3C_6H_2$–	84	81
9g	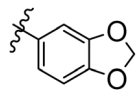	77	76

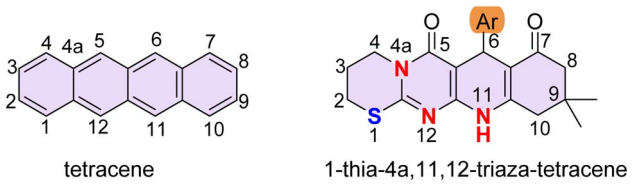

Fig. 4 General structure of the newly synthesized tetracyclic heterocycles classified as thiaza-tetracene framework.

to the cell wall, alterations in the metabolism of carbohydrates, fatty acids, or amino acids, interference with DNA replication, inhibition of the protein involved in cell division, and inhibition of the tyrosine phosphatase protein involved in gene transcription. Methoxy groups are essential for improving the antimicrobial activity of compounds.[76] Compound **9b** (with chlorine) was inactive against *E. coli* and *E. faecalis*. This indicates that the mere presence of a halogen is not sufficient; its effect is heavily dependent on its position and the overall molecular scaffold, influencing both steric and electronic properties.[77] Conversely, one group of compounds (**9d**, **9b**) was

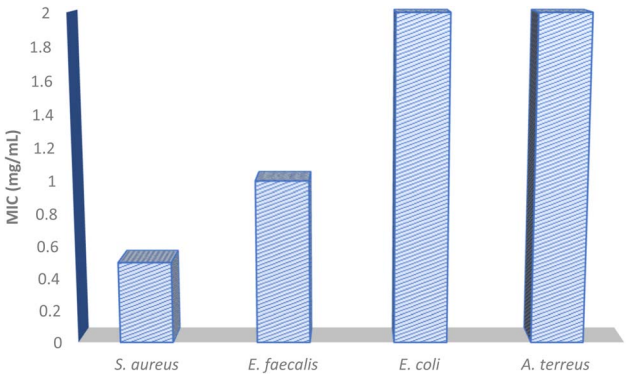

Fig. 5 Minimum Inhibitory Concentration (MIC) of compound **9a**.

inactive against two bacterial strains, while another group (**9c**, **9e**, **9g**) showed no activity solely against *A. terreus*.[75]

Measurement of minimum inhibitory concentration (MIC)

The minimum inhibitory concentration (MIC) of compound **9a** was determined against the four microbial strains (Fig. 5). The compound demonstrated superior potency against *S. aureus* (MIC = 0.5 mg mL^{-1}), followed by *E. faecalis* (MIC = 1 mg mL^{-1}), while *E. coli* and *A. terreus* were inhibited at a higher concentration of 2 μg mL^{-1}.

Molecular docking

The primary goal of antimicrobial discovery is to identify compounds with a broad spectrum of activity and high potency. Based on these criteria, compound **9a** emerges as the most promising candidate. Modeling studies were employed to investigate the binding interactions of the compound **9a** and the reference drugs (tetracycline for bacteria and fluconazole for fungi) with the active site of the target protein. Molecular docking was performed against DNA-directed RNA polymerase from *Staphylococcus aureus* (Q2FW32) as a bacterial protein, and *A. terreus* (A0A5M3YQC0) as a fungal protein, as shown in Table 3. DNA-directed RNA polymerase was selected as a putative target in this study due to its well-established role as a crucial

Table 2 Antimicrobial activity represented by the inhibition zone (mm) of the tested compounds at a 1 mg per mL concentration[a]

Compounds (1 mg mL^{-1})	Bacterial strains			Fungal strains
	S. aureus	*E. faecalis*	*E. coli*	*A. terreus*
9d	$7^{b} \pm 0$	$0^{a} \pm 0$	$0^{a} \pm 0$	$2.33^{a} \pm 4.04$
9c	$0^{a} \pm 0$	$2.33^{ab} \pm 4.04$	$7.33^{c} \pm 0.58$	$0^{a} \pm 0$
9b	$2.33^{a} \pm 4.04$	$0^{a} \pm 0$	$0^{a} \pm 0$	$2.33^{a} \pm 4.04$
9e	$9^{b} \pm 1$	$2.33^{ab} \pm 4.04$	$4.67^{bc} \pm 4.04$	$0^{a} \pm 0$
9a	$9.67^{b} \pm 1.53$	$7^{bc} \pm 1$	$2.33^{ab} \pm 4.04$	$4.67^{a} \pm 4.04$
9f	$0^{a} \pm 0$	$2.33^{ab} \pm 4.04$	$8.67^{c} \pm 0.58$	$2.33^{a} \pm 4.04$
9g	$8.33^{b} \pm 1.53$	$8^{d} \pm 1$	$8.33^{c} \pm 1.53$	$0^{a} \pm 0$
Positive control	$17^{c} \pm 2.65$	$13.33^{e} \pm 1.53$	$17.33^{d} \pm 2.52$	$13.67^{b} \pm 1.53$
LSD 5%	2.42	2.08	2.45	2.10

[a] Data are expressed as mean ± standard deviation ($n = 3$). Different lowercase letters within the same column indicate statistically significant differences ($p < 0.05$). The positive control (tetracycline for bacteria and fluconazole for fungi) was used.

Table 3 Molecular docking results and binding energies of compound **9a** and reference controls (tetracycline and fluconazole) against the DNA-directed RNA polymerase (RNAP) of specific microbial targets

Microbial target	RNAP subunit (PDB ID)	Ligand	Binding energy (ΔG, kcal mol^{-1})	No. of interactions	Key interaction types	Key residues involved
S. aureus (bacterial protein)	Q2FW32	Compound **9a**	−6.7	11	Pi–anion, pi–sigma, alkyl bond	GLU208, LEU212
		Tetracycline	−6.4	5	Conventional hydrogen, pi–sigma, amide–pi stacked, pi–alkyl bond	GLY50, ALA51, LYS88, SER203, TYR90
A. terreus (fungal protein)	A0A5M3YQC0	Compound **9a**	−9.2	10	Conventional hydrogen, carbon–hydrogen, pi–alkyl bond	LYS112, IEL115, ARG218, PRO242, LEU110, LYS106
		Fluconazole	−7	11	Conventional hydrogen, carbon–hydrogen, halogen, (fluorine), amide–pi stacked, pi–alkyl bond	TYR527, PRO242, ASP241, LEU531, VAL111, LYS112, LEU110, GLY109, LEU105

target for antibacterial drug discovery. This is evidenced by the clinical success of several antibiotics, such as rifampicin and fidaxomicin, which specifically inhibit bacterial RNA polymerase to achieve their therapeutic effects.[78] This validates RNAP as a high-value target for screening novel antimicrobial compounds. These findings suggest that RNAP could be considered a promising putative target for the screening of novel antimicrobial compounds.

As shown in Fig. 6, molecular docking against *S. aureus* DNA-directed RNA polymerase was performed to investigate a potential mechanism of action. The results revealed an intriguing contrast between the *in silico* and *in vitro* activities. Compound **9a** demonstrated a strong predicted binding affinity with a free binding energy (ΔG) of −6.7 kcal mol^{-1}. It formed three interactions, including key bonds with residues GLU208 and LEU212. In contrast, the reference control, tetracycline, showed a comparably weak predicted binding (ΔG =

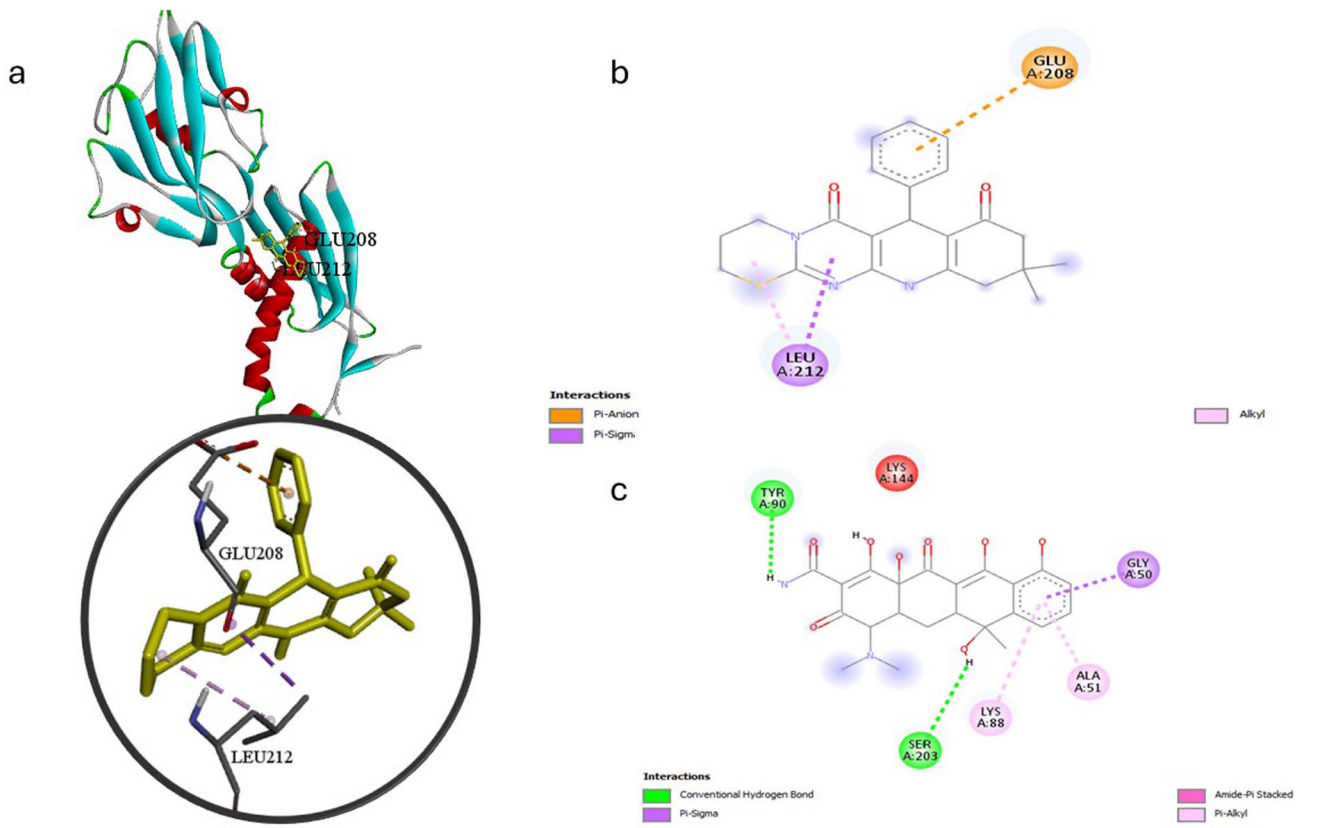

Fig. 6 (a) 3D molecular docking visualization of compound **9a** within the active site of *S. aureus* DNA-directed RNA polymerase (RNAP) (PDB Q2FW32) as a bacterial protein. The inset shows a zoomed-in view highlighting the key binding interactions within the catalytic pocket. (b) 2D ligand–protein interaction diagram of compound **9a**. (c) 2D ligand–protein interaction diagram of reference control (tetracycline).

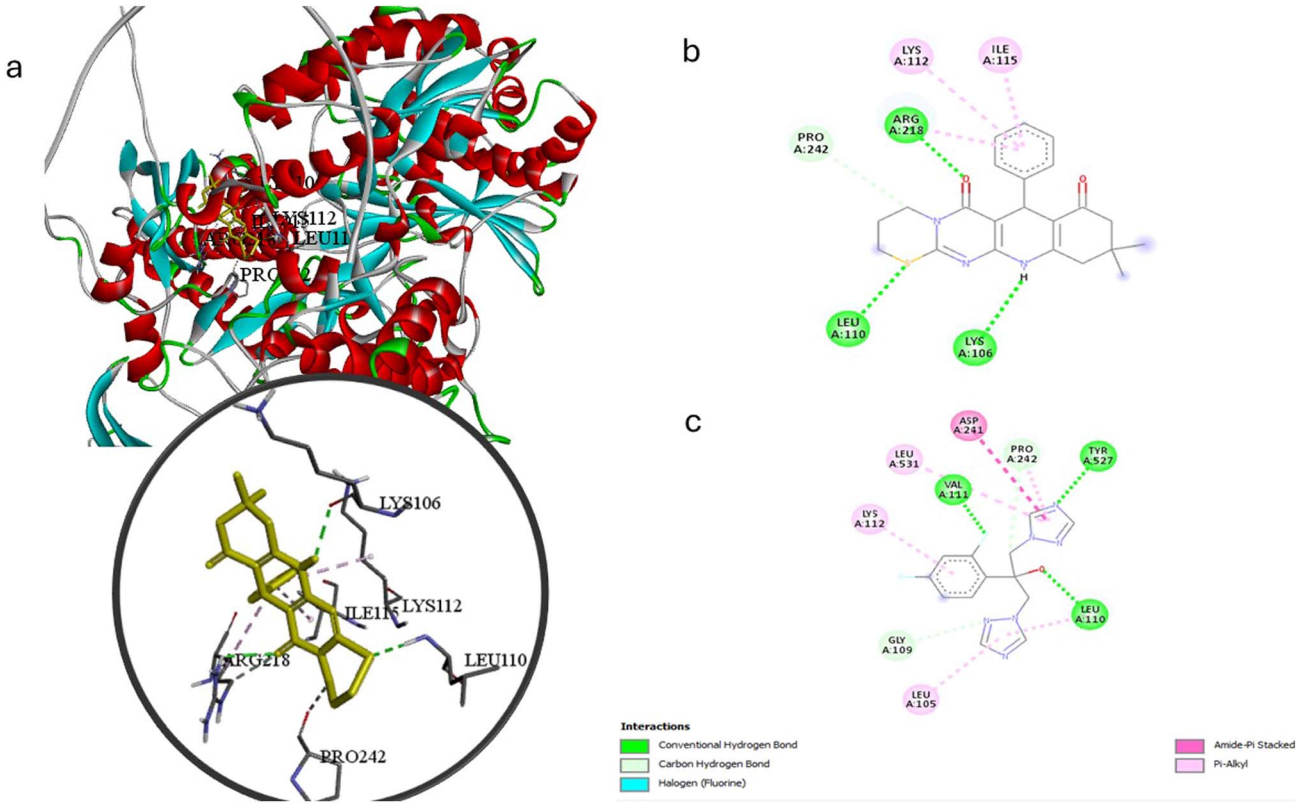

Fig. 7 (a) 3D molecular docking visualization of compound **9a** within the active site of *A. terreus* DNA-directed RNA polymerase (RNAP) (PDB A0A5M3YQC0). The inset shows a zoomed-in view highlighting the key binding interactions within the catalytic pocket. (b) 2D ligand–protein interaction diagram of compound **9a**. (c) 2D ligand–protein interaction diagram of reference control (fluconazole).

−6.4 kcal mol^{-1}) with five interactions with the same target protein. Compound **9a** displayed a superior predicted binding affinity compared to tetracycline. Since tetracycline is *in vitro* more potent against *S. aureus*, this discrepancy strongly suggests that the primary antibacterial effect of tetracycline is not mediated through RNA polymerase inhibition,[79] which is consistent with its well-established mechanism of inhibiting protein synthesis by binding to the 30S ribosomal subunit.[80] The weak binding of tetracycline to RNAP in our simulation is consistent with its reported mechanism of action, suggesting limited interaction with this target *in silico*. Conversely, the stronger predicted binding of compound **9a** to RNAP may not necessarily reflect its actual intracellular target *in vivo*, as docking results alone cannot confirm biological activity. Overall, the docking analysis suggests that compound **9a** and tetracycline may exhibit different binding profiles toward RNAP, warranting further experimental validation to clarify their mechanisms of action.

Compound **9a** demonstrated a significantly superior predicted binding affinity (−9.2 kcal mol^{-1}) against *A. terreus* compared to the clinical antifungal fluconazole (−7.0 kcal mol^{-1}). While fluconazole formed more interactions, the diverse profile of compound **9a**, including critical conventional hydrogen, carbon-hydrogen, and strong hydrophobic pi–alkyl interactions with key catalytic residues like LYS112, IEL115, ARG218, PRO242, LEU110, and LYS106, is likely responsible for its superior predicted affinity (Fig. 7). Hydrophobic interactions are known to provide major entropic gains,[81] and hydrogen bonds to key active site residues are particularly effective for stabilization.[82]

However, the most plausible explanation for the reduced experimental activity involves suboptimal cellular permeability or susceptibility to bacterial efflux pumps, which can prevent the compound from reaching its intracellular target at sufficient concentration. Consequently, these findings suggest that compound **9a** may represent a promising lead structure due to its predicted strong binding affinity, while clearly directing future optimization efforts towards enhancing its physicochemical properties for improved cellular delivery. The physicochemical profile of a compound, such as its molecular weight, lipophilicity, and polarity, is a critical determinant of its ability to traverse the bacterial cell envelope and reach its intracellular target at a sufficient concentration.[83] Furthermore, the potential involvement of bacterial efflux pumps, which are known to reduce intracellular drug accumulation significantly, cannot be ruled out.[84] A key limitation of this work is the reliance on *in silico* docking studies without complementary *in vitro* enzymatic assays to confirm the proposed molecular target.

Conclusion

In summary, we have developed a novel and efficient synthetic strategy for the construction of tetracyclic heterocycles, namely 1-thia-4*a*,11,12-triaza-tetracenes. To the best of our knowledge,

this fused framework has not been previously reported, thereby representing a new class of heterocyclic systems. The methodology is based on the use of 8-amino-3,4-dihydropyrimido[2,1-*b*][1,3]thiazin-6-one as a key enamine building block in a one-pot multicomponent reaction with aldehydes and dimedone, providing a concise and convergent route to structurally complex tetracyclic architectures. Compared with previously reported approaches, this protocol offers notable advantages, including operational simplicity, good yields, and access to structurally diverse products. The assigned structures were unambiguously confirmed through alternative synthetic pathways and detailed HMBC spectroscopic analysis.

Biological evaluation demonstrated that several of the synthesized compounds exhibit promising antimicrobial activity, with compound **9a** emerging as the most potent derivative, particularly against *Staphylococcus aureus*. Molecular docking studies further supported these results, revealing favorable binding affinities of compound **9a** toward both fungal and bacterial targets, exceeding those of reference drugs such as fluconazole and tetracycline.

Overall, the present study highlights the potential of this newly developed tetracyclic scaffold as a valuable platform for antimicrobial drug discovery. Further structural optimization and experimental validation, including enzymatic studies, are recommended to confirm the proposed mechanism and fully explore its therapeutic potential.

Materials and methods

Chemistry

"Melting points were measured using a Stuart melting point apparatus and were uncorrected. The IR spectra were recorded using an FTIR Bruker-Vector 22 spectrophotometer using KBr pellets. The ^{1}H and ^{13}C NMR spectra were recorded in DMSO-d_6 as a solvent with a Varian Mercury VXR-300 NMR spectrometer operating at 300 MHz and 75 MHz, or a Bruker AVS NMR spectrometer at 500 MHz and 125 MHz, respectively, using TMS as an internal standard. Chemical shifts were reported as δ values in ppm. Mass spectra were recorded with a Shimadzu GCMS-QP-1000 EX mass spectrometer in EI (70 eV) mode. The elemental analyses were performed at the Micro Analytical Centre, Cairo University, and Helwan University.

General method for the synthesis of (5)

A solution of 6-amino-2-thioxo-2,3-dihydropyrimidin-4(1*H*)-one (**1**) (143 mg, 1 mmol) and KOH (112 mg, 2 mmol) in EtOH (10 mL) was boiled for 10 min. Then 1,3-dibromopropane (**2**) (102 mL, 1 mmol) was added to the resulting potassium salt. The reaction mixture was refluxed for 7 hours. Thereupon, the mixture was poured over crushed ice, and the formed precipitate was filtered off, dried, and then recrystallized from ethanol.

8-Amino-3,4-dihydro-2*H*,6*H*-pyrimido[2,1-*b*][1,3]thiazin-6-one (5). Pale yellow crystals (147 mg, 90%); mp 257–260 °C; IR (KBr): $\bar{\nu}$ 3450 (NH_2), 1695 (C=O), 1615 (C=N) cm^{-1}; ^{1}H NMR (300 MHz, DMSO-d_6) δ 2.03–2.11 (m, 2H, CH_2), 3.13 (t, J = 5.9 Hz, 2H, CH_2), 3.81 (t, J = 5.7 Hz, 2H, CH_2), 4.90 (s, 1H, C*H*), 6.34 (s, 2H, NH_2) ppm. MS (El, 70 eV): *m*/*z* (%) 183 [M$^+$] anal. calcd for $C_7H_9N_3OS$: C, 45.89; H, 4.95; N, 22.93. Found: C, 45.73; H, 4.77; N, 22.74%.

General method for the synthesis of 9a–g

Method A. In an acetic acid (10 mL), a solution of 8-amino-3,4-dihydro-2*H*,6*H*-pyrimido[2,1-*b*][1,3]thiazin-6-one (**5**) (183 mg, 1 mmol), dimedone (**7**) (140 mg, 1 mmol), and the appropriate aldehydes **8a–g** (1 mmol) was heated at reflux for 7 h. The solvent was evaporated, and the formed precipitate was filtered from ethanol and recrystallized from EtOH/DMF [1 : 3] mixture to give the titled compound.

Method B. To a solution of 5-aryl-2-thioxohexahydropyrimido[4,5-*b*]quinoline-4,6-diones (**18a–g**) (obtained *via* a three component reaction) (1 mmol) and KOH (112 mg, 2 mmol) in EtOH (10 mL) was boiled for 10 min. 1,3-Dibromopropane (**2**) (102 mL, 1 mmol), was added to the resulting potassium salt. The reaction mixture was refluxed for 7 hours. Thereupon, the mixture was poured over crushed ice, and the formed precipitate was filtered off, dried, and then recrystallized from an EtOH/DMF [1 : 3] mixture to give the titled compound.

*10,10-Dimethyl-7-phenyl-3,4,7,10,11,12-hexahydro-2H,6H-[1,3]thiazino[3′,2′:1,2]pyrimido[4,5-b]quinoline-6,8(9H)-dione (**9a**).* Colorless powder (method A: 77%, method B: 69%); mp > 300 °C; IR (KBr): $\bar{\nu}$ 3236 (N*H*), 1668 (C=O), 1616 (C=N), 1516 (C=C) cm^{-1}; ^{1}H NMR (500 MHz, DMSO-d_6) δ 0.90 (s, 3H, CH_3), 1.00 (s, 3H, CH_3), 1.98–2.19 (m, 4H, 2CH_2), 2.36–2.47 (m, 2H, CH_2), 3.12–3.18 (m, 2H, CH_2), 3.67–3.91 (m, 2H, CH_2), 4.88 (s, 1H, *H*7), 7.06 (t, J = 6.7 Hz, 1H, Ar–*H*), 7.18 (d, J = 6.5 Hz, 4H, Ar–*H*), 9.88 (s, 1H, N*H*) ppm; ^{13}C NMR (125 MHz, DMSO-d_6): δ 22.4, 27.2, 27.4, 29.3, 32.6, 34.9, 41.6, 50.7, 97.8, 110.0, 126.3, 128.1, 128.2, 147.0, 150.9, 151.4, 158.5, 160.6, 194.3 ppm; MS (El, 70 eV): *m*/*z* (%) 393 [M$^+$] anal. calcd for $C_{22}H_{23}N_3O_2S$: C, 67.15; H, 5.89; N, 10.68. Found: C, 66.97; H, 5.71; N, 10.57%.

*7-(4-Chlorophenyl)-10,10-dimethyl-3,4,7,10,11,12-hexahydro-2H,6H-[1,3]thiazino[3′,2′:1,2]pyrimido[4,5-b]quinoline-6,8(9H)-dione (**9b**).* Yellow powder (method A: 87%, method B: 84%); mp > 300 °C; IR (KBr): $\bar{\nu}$ 3236 (N*H*), 1657 (C=O), 1603 (C=N), 1509 (C=C) cm^{-1}; ^{1}H NMR (300 MHz, DMSO-d_6) δ 0.89 (s, 3H, CH_3), 0.99 (s, 3H, CH_3), 1.97–2.14 (m, 4H, 2CH_2), 2.41 (br.s, 2H, CH_2), 3.14 (t, J = 6.0 Hz, 2H, CH_2), 3.73–3.92 (m, 2H, CH_2), 4.86 (s, 1H, *H*7), 7.17–7.24 (m, 4H, Ar–*H*), 9.85 (s, 1H, N*H*) ppm; ^{13}C NMR (125 MHz, DMSO-d_6): δ 22.4, 27.3, 27.4, 29.3, 32.6, 34.7, 41.6, 50.6, 97.4, 109.7, 128.2, 130.0, 130.8, 146.0, 150.9, 151.6, 158.9, 160.5, 194.4 ppm; MS (El, 70 eV): *m*/*z* (%) 427 [M$^+$] anal. calcd for $C_{22}H_{22}ClN_3O_2S$: C, 61.75; H, 5.18; N, 9.82. Found: C, 61.64; H, 5.03; N, 9.70%.

*10,10-Dimethyl-7-(p-tolyl)-3,4,7,10,11,12-hexahydro-2H,6H-[1,3]thiazino[3′,2′:1,2]pyrimido[4,5-b]quinoline-6,8(9H)-dione (**9c**).* Colorless powder (method A: 82%, method B: 75%); mp > 300 °C; IR (KBr): $\bar{\nu}$ 3224 (N*H*), 1670 (C=O), 1617 (C=N), 1516 (C=C) cm^{-1}; ^{1}H NMR (500 MHz, DMSO-d_6) δ 0.83 (s, 3H, CH_3), 0.93 (s, 3H, CH_3), 1.90–2.07 (m, 4H, 2CH_2), 2.12 (s, 3H, CH_3), 2.29–2.40 (m, 2H, CH_2), 3.07–3.10 (m, 2H, CH_2), 3.69–3.83 (m, 2H, CH_2), 4.77 (s, 1H, *H*7), 6.90 (d, J = 7.7 Hz, 2H, Ar–*H*), 7.00 (d, J =

7.7 Hz, 2H, Ar–*H*), 9.75 (s, 1H, N*H*) ppm; ^{13}C NMR (125 MHz, DMSO-d_6): δ 21.0, 22.4, 27.2, 27.4, 29.4, 32.6, 34.4, 41.5, 50.6, 98.0, 110.1, 128.0, 128.7, 135.2, 144.2, 150.8, 151.2, 158.4, 160.5, 194.4 ppm; MS (El, 70 eV): *m*/*z* (%) 407 [M$^+$] anal. calcd for $C_{23}H_{25}N_3O_2S$: C, 67.79; H, 6.18; N, 10.31. Found: C, 67.69; H, 6.03; N, 10.26%.

*7-(4-Methoxyphenyl)-10,10-dimethyl-3,4,7,10,11,12-hexahydro-2H,6H-[1,3]thiazino[3′,2′:1,2]pyrimido[4,5-b]quinoline-6,8(9H)-dione (**9d**).* Pale yellow powder (method A: 87%, method B: 79%); mp > 300 °C; IR (KBr): $\bar{\nu}$ 3251 (N*H*), 1633 (C=O), 1585 (C=N), 1506 (C=C) cm^{-1}; ^{1}H NMR (500 MHz, DMSO-d_6) δ 0.87 (s, 3H, CH_3), 0.97 (s, 3H, CH_3), 1.97–2.11 (m, 6H, 3CH_2), 3.12 (br.s, 2H, CH_2), 3.64 (s, 3H, OCH_3), 3.86 (br.s, 2H, CH_2), 5.0 (s, 1H, *H*7), 6.70 (br.s, 2H, Ar–*H*), 7.05 (br.s, 2H, Ar–*H*), 9.78 (s, 1H, N*H*) ppm; MS (El, 70 eV): *m*/*z* (%) 423 [M$^+$] anal. calcd for $C_{23}H_{25}N_3O_3S$: C, 65.23; H, 5.95; N, 9.92. Found: C, 65.10; H, 5.78; N, 9.75%.

*10,10-Dimethyl-7-(4-nitrophenyl)-3,4,7,10,11,12-hexahydro-2H,6H-[1,3]thiazino[3′,2′:1,2]pyrimido[4,5-b]quinoline-6,8(9H)-dione (**9e**).* Pale yellow powder (method A: 85%, method B: 81%); mp 245–247 °C; IR (KBr): $\bar{\nu}$ 3248 (N*H*), 1645 (C=O), 1554 (C=N), 1510 (C=C) cm^{-1}; ^{1}H NMR (300 MHz, DMSO-d_6) δ 0.89 (s, 3H, CH_3), 1.00 (s, 3H, CH_3), 1.97–2.12 (m, 4H, 2CH_2), 2.16–2.45 (m, 2H, CH_2), 3.15 (t, J = 6.0 Hz, 2H, CH_2), 3.72–3.92 (m, 2H, CH_2), 4.97 (s, 1H, *H*7), 7.46 (d, J = 8.2 Hz, 2H, Ar–*H*), 8.07 (d, J = 8.4 Hz, 2H, Ar–*H*), 9.97 (s, 1H, N*H*) ppm; ^{13}C NMR (125 MHz, DMSO-d_6) δ 21.7, 27.5, 29.7, 32.4, 35.2, 41.3, 42.8, 52.2, 97.6, 110.4, 121.5, 127.3, 140.3, 147.5, 151.7, 152.3, 155.5, 162.4, 194.5 ppm; MS (El, 70 eV): *m*/*z* (%) 438 [M$^+$] anal. calcd for $C_{22}H_{22}N_4O_4S$: C, 60.26; H, 5.06; N, 12.78. Found: C, 60.15; H, 4.92; N, 12.59%.

*10,10-Dimethyl-7-(3,4,5-trimethoxyphenyl)-3,4,7,10,11,12-hexahydro-2H,6H-[1,3]thiazino[3′,2′:1,2]pyrimido[4,5-b]quinoline-6,8(9H)-dione (**9f**).* Colorless powder (method A: 84%, method B: 81%); mp > 300 °C; IR (KBr): $\bar{\nu}$ 3228 (N*H*), 1665 (C=O), 1615 (C=N), 1514 (C=C) cm^{-1}; ^{1}H NMR (300 MHz, DMSO-d_6) δ 0.99 (s, 3H, CH_3), 1.03 (s, 3H, CH_3), 2.02–2.18 (m, 4H, 2CH_2), 2.45 (br.s, 2H, CH_2), 3.15 (t, J = 6.2 Hz, 2H, CH_2), 3.58 (s, 3H, OCH_3), 3.67 (s, 6H, 2OCH_3), 3.84–3.90 (m, 2H, CH_2), 4.87 (s, 1H, *H*7), 6.50 (s, 2H, Ar–*H*), 9.80 (s, 1H, N*H*) ppm; ^{13}C NMR (125 MHz, DMSO-d_6) δ 21.4, 27.2, 27.5, 29.4, 32.4, 34.8, 41.6, 42.1, 52.5, 56.9, 59.6, 98.2, 106.6, 110.5, 136.2, 137.5, 148.4, 152.4, 157.5, 159.4, 162.5, 194.7 ppm; MS (El, 70 eV): *m*/*z* (%) 483 [M$^+$] anal. calcd for $C_{25}H_{29}N_3O_5S$: C, 62.09; H, 6.04; N, 8.69. Found: C, 61.90; H, 5.89; N, 8.53%.

*7-(Benzo[d][1,3]dioxol-5-yl)-10,10-dimethyl-3,4,7,10,11,12-hexahydro-2H,6H-[1,3]thiazino[3′,2′:1,2]pyrimido[4,5-b]quinoline-6,8(9H)-dione (**9g**).* Creamy powder (method A: 77%, method B: 76%); mp > 300 °C; ^{1}H NMR (500 MHz, DMSO-d_6) δ 0.92 (s, 3H, CH_3), 1.00 (s, 3H, CH_3), 2.01–2.19 (m, 4H, 2CH_2), 2.37–2.46 (m, 2H, CH_2), 3.16 (t, J = 6.0 Hz, 2H, CH_2), 3.79–3.92 (m, 2H, CH_2), 4.81 (s, 1H, *H*7), 5.91 (s, 2H, –OCH_2O–), 6.62 (d, J = 8.1 Hz, 1H, Ar–*H*), 6.70–6.73 (m, 2H, Ar–*H*), 9.87 (s, 1H, N*H*) ppm; ^{13}C NMR (125 MHz, DMSO-d_6): δ 21.5, 22.4, 27.3, 29.3, 32.7, 34.5, 41.6, 50.7, 97.9, 101.0, 108.1, 108.7, 110.0, 120.8, 141.2, 145.7, 147.1, 150.8, 151.3, 158.5, 160.6, 194.4 ppm; MS (El, 70 eV): *m*/*z* (%) 437 [M$^+$] anal. calcd for $C_{23}H_{23}N_3O_4S$: C, 63.14; H, 5.30; N, 9.60. Found: C, 62.98; H, 5.19; N, 9.45%.

Antimicrobial study

The Gram-positive bacteria, including *Enterococcus faecalis* ATCC 29212, and *Staphylococcus aureus* ATCC 29213, Gram-negative bacteria such as *Escherichia coli* ATCC 35218, and fungal species, including *Aspergillus terreus*, were used to measure the antimicrobial activity of the synthesized compound at a 1 mg per mL concentration against bacterial and fungal strains by the disc-diffusion method. Tetracycline and fluconazole were used as positive controls for bacterial and fungal species, respectively, while DMSO was used as a negative control. The inhibition zone diameter was measured in mm. This experiment was carried out in triplicate.[85,86]

Determination of minimum inhibitory concentration (MIC)

The minimum inhibitory concentration (MIC) of the compound was evaluated against bacterial and fungal strains using broth microdilution and agar dilution methods, respectively. For bacteria, two-fold serial dilutions of the compound (0.125–4 mg mL^{-1}) in nutrient broth were inoculated with a standardized bacterial suspension (~1.5 × 10^6 CFU mL^{-1}) in a 96-well plate. Following incubation at 37 °C for 18–24 h, resazurin indicator (0.675 mg mL^{-1}) was added. The MIC was defined as the lowest concentration preventing a color change from blue to pink. For fungi, the compound was incorporated into agar plates at the same concentration range. After inoculation, the plates were incubated at 27 °C for 7 days, and the MIC was recorded as the lowest concentration completely inhibiting visible growth compared to the control.[87,88]

Molecular docking

The molecular docking was performed using AutoDock Vina 1.5.7 to predict the binding modes and affinities of the most active compound and the reference drugs (tetracycline and fluconazole) against DNA-directed RNA polymerase (RNAP).[89] The crystal structures of the RNAP from *Staphylococcus aureus* (Q2FW32) as a bacterial protein, and *A. terreus* (A0A5M3YQC0) as a fungal protein, were obtained from the Protein Data Bank (PDB) *via* their UniProt IDs. These protein structures were pre-processed by removing water molecules, adding polar hydrogen atoms, and assigning Gasteiger charges.[90] The binding pockets were identified using CB-DOCK2.[91] The resulting protein–ligand complexes were visualized and analyzed using BIOVIA Discovery Studio Visualizer 2021 to determine the binding energies (ΔG, kcal mol^{-1}) and key intermolecular interactions, such as hydrogen bonds and hydrophobic contacts.[92]

Statistical analysis

All antimicrobial activity assays were conducted in triplicate, and results are presented as mean ± standard deviation. Statistical significance was determined using one-way ANOVA followed by Duncan's multiple range test in SPSS (version 21), with $P < 0.05$ considered significant.[93]

Conflicts of interest

There are no conflicts of interest to declare.

Data availability

The data supporting this study are available from the corresponding author upon reasonable request.

Supplementary information (SI): ^{1}H NMR and ^{13}C NMR spectra. See DOI: https://doi.org/10.1039/d6ra03008d.

Acknowledgements

This work was supported and funded by the Deanship of Scientific Research at Imam Mohammad Ibn Saud Islamic University (IMSIU) (grant number IMSIU-DDRSP2601).

References

1 T. A. Abdallah, A. M. Salaheldin and N. F. Radwan, *Z. Naturforsch., B:J. Chem. Sci.*, 2007, **62**, 261–266.
2 S. Mondal, *ChemistrySelect*, 2025, **10**, e202501194.
3 A. Z. A. Elassar and A. A. El-Khair, *Tetrahedron*, 2003, **59**, 8463–8480.
4 A. Y. Sukhorukov, *Synlett*, 2020, **31**, 439–449.
5 N. R. Candeias, F. Montalbano, P. M. S. D. Cal and P. M. P. Gois, *Chem. Rev.*, 2010, **110**, 6169–6193.
6 N. Isambert, M. del, M. S. Duque, J.-C. Plaquevent, Y. Génisson, J. Rodriguez and T. Constantieux, *Chem. Soc. Rev.*, 2011, **40**, 1347–1357.
7 M. Shiri, *Chem. Rev.*, 2012, **112**, 3508–3549.
8 A. Dömling, W. Wang and K. Wang, *Chem. Rev.*, 2012, **112**, 3083–3135.
9 S. Brauch, S. S. van Berkel and B. Westermann, *Chem. Soc. Rev.*, 2013, **42**, 4948–4962.
10 M. N. Chen, L. P. Mo, Z. S. Cui and Z. H. Zhang, *Curr. Opin. Green Sustainable Chem.*, 2019, **15**, 27–37.
11 M. Zhang, Y. H. Liu, Z. R. Shang, H. C. Hu and Z. H. Zhang, *Catal. Commun.*, 2017, **88**, 39–44.
12 C. Safak and R. Simsek, *Mini-Rev. Med. Chem.*, 2006, **6**, 747–755.
13 J. Wollmann, C. Baumert, G. Erlenkamp, W. Sippl and A. Hilgeroth, *ChemBioChem*, 2008, **9**, 874–878.
14 Y. L. N. Murthy, A. Rajack, M. T. Ramji, J. J. Babu, Ch. Praveen and K. A. Lakshmic, *Bioorg. Med. Chem. Lett.*, 2012, **22**, 6016–6023.
15 S. J. Choi, J. H. Cho, I. Im, S. D. Lee, J. Y. Jang, Y. M. Oh, Y. K. Jung, E. S. Jeon and Y. C. Kim, *Eur. J. Med. Chem.*, 2010, **45**, 2578–2590.
16 J. M. Tusell, S. Barrón and J. Serratosa, *Brain Res.*, 1993, **622**, 99–104.
17 A. Kolocouris, K. Dimas, C. Pannecouque, M. Witvrouw, G. B. Foscolos, G. Stamatiou, G. Fytas, G. Zoidis, N. Kolocouris, G. Andrei, R. Snoeck and E. De Clercq, *Bioorg. Med. Chem. Lett.*, 2002, **12**, 723–727.
18 J. M. Quintela, C. Peinador, L. Botana, M. Estévez and R. Riguera, *Bioorg. Med. Chem.*, 1997, **5**, 1543–1553.
19 A. S. Girgis, H. M. Hosni and I. S. Ahmed-Farag, *Z. Naturforsch. B*, 2003, **58**, 678–685.
20 A. E. Amr and M. M. Abdulla, *Bioorg. Med. Chem.*, 2006, **14**, 4341–4352.
21 J.-K. Son, L.-X. Zhao, A. Basnet, P. Thapa, R. Karki, Y. Na, Y. Jahng, T. C. Jeong, B.-S. Jeong, C.-S. Lee and E.-S. Lee, *Eur. J. Med. Chem.*, 2008, **43**, 675–682.
22 F. Xie, H. Zhao, L. Zhao, L. Lou and Y. Hu, *Bioorg. Med. Chem. Lett.*, 2009, **19**, 275–278.
23 V. Pathak, H. K. Maurya, S. Sharma, K. K. Srivastava and A. Gupta, *Bioorg. Med. Chem. Lett.*, 2014, **24**, 2892–2896.
24 M. A. Abdelgawad, R. B. Bakr and A. A. Azouz, *Bioorg. Chem.*, 2018, **77**, 339–348.
25 H. M. Diab, M. E. Salem, I. A. Abdelhamid and A. H. M. Elwahy, *ARKIVOC*, 2021, 329–377.
26 E. Carosati, R. Mannhold, P. Wahl, J. B. Hansen, T. Fremming, I. Zamora, G. Cianchetta and M. Baroni, *J. Med. Chem.*, 2007, **50**, 2117–2126.
27 A. A. Joshi and C. L. Viswanathan, *Bioorg. Med. Chem. Lett.*, 2006, **16**, 2613–2617.
28 N. Muruganantham, R. Sivakumar, N. Anbalagan, V. Gunasekaran and J. T. Leonard, *Biol. Pharm. Bull.*, 2004, **27**, 1683–1687.
29 P. Narender, U. Srinivas, M. Ravinder, B. A. Rao, C. Ramesh, K. Harakishore, B. Gangadasu, U. S. N. Murthy and V. J. Rao, *Bioorg. Med. Chem.*, 2006, **14**, 4600–4609.
30 R. G. Ridley, *Nature*, 2002, **415**, 686.
31 A. Tsotinis, M. Vlachou, S. Zouroudis, A. Jeney, F. Timár, D. E. Thurston and C. Roussakis, *Lett. Drug Des. Discovery*, 2005, **2**, 189–192.
32 A. B. A. El-Gazzar, H. N. Hafez and G. A. M. Nawwar, *Eur. J. Med. Chem.*, 2009, **44**, 1427–1436.
33 E. Rajanarendar, M. N. Reddy, S. R. Krishna, K. R. Murthy, Y. N. Reddy and M. V. Rajam, *Eur. J. Med. Chem.*, 2012, **55**, 273–283.
34 L. Cordeu, E. Cubedo, E. Bandrés, A. Rebollo, X. Sáenz, H. Chozas, M. V. Domínguez, M. Echeverría, B. Mendivil, C. Sanmartin and J. A. Palop, *Bioorg. Med. Chem.*, 2007, **15**, 1659–1669.
35 S. I. Alqasoumi, A. M. Al-Taweel, A. M. Alafeefy, E. Noaman and M. M. Ghorab, *Eur. J. Med. Chem.*, 2010, **45**, 738–744.
36 B. Insuasty, D. Becerra, J. Quiroga, R. Abonia, M. Nogueras and J. Cobo, *J. Heterocycl. Chem.*, 2013, **50**, 506–512.
37 M. M. Ghorab, F. Ragab, H. I. Heiba, R. K. Arafa and E. M. El-Hossary, *Eur. J. Med. Chem.*, 2010, **45**, 3677–3684.
38 S. T. Selvi, V. Nadaraj, S. Mohan, R. Sasi and M. Hema, *Bioorg. Med. Chem.*, 2006, **14**, 3896–3903.
39 E. Rajanarendar, M. N. Reddy, S. R. Krishna, K. R. Murthy, Y. N. Reddy and M. V. Rajam, *Eur. J. Med. Chem.*, 2012, **55**, 273–283.
40 A. R. B. A. El-Gazzar, M. M. El-Enany and M. N. Mahmoud, *Bioorg. Med. Chem.*, 2008, **16**, 3261–3273.
41 F. W. Muregi and A. Ishih, *Drug Dev. Res.*, 2009, **71**, 20–32.
42 K. Singh, H. Kaur, P. Smith, C. de Kock, K. Chibale and J. Balzarini, *J. Med. Chem.*, 2014, **57**, 435–448.
43 C. Viegas-Junior, E. J. Barreiro and C. A. M. Fraga, *Curr. Med. Chem.*, 2007, **14**, 1829–1852.

44 H. M. Diab, M. E. Salem, M. Abdellatif, M. M. Soliman, I. A. Abdelhamid, A. H. M. Elwahy, N. Raza and Y. A. El-Gabry, *ACS Omega*, 2025, **10**, 38014–38033.
45 H. M. Diab, D. H. Ali, T. A. Abdallah, M. M. Soliman, A. H. M. Elwahy, I. A. Abdelhamid, M. E. Salem and I. M. Z. Fares, *J. Heterocycl. Chem.*, 2025, **62**, 1679–1697.
46 H. H. Mohamed, M. E. Salem, E. B. Abdelazim, A. M. Abdelmoniem, M. Elsabahy, N. Raza, A. H. Abdullah and I. A. Abdelhamid, *ACS Omega*, 2025, **10**, 46868–46883.
47 M. A. Ragheb, M. E. Salem, M. M. Ali, I. A. Abdelhamid, N. Raza and M. H. Soliman, *ACS Omega*, 2025, **43**, 51497–51511.
48 M. E. Salem, M. A. Ragheb, A. H. Abdullah, M. N. Goda, I. A. Abdelhamid and A. H. M. Elwahy, *J. Mol. Struct.*, 2026, **1350**, 144064.
49 H. M. Diab, M. E. Salem, A. H. M. Elwahy, M. A. Ragheb, M. A. Noamaan, F. K. Algethami, I. A. Abdelhamid and H. K. Mahmoud, *RSC Adv.*, 2026, **16**, 7389–7409.
50 M. R. Alsulami, M. E. Salem, I. A. Abdelhamid, A. H. M. Elwahy, K. Barakat, A. M. Abdelmoniem, N. Raza and R. E. Abdelwahab, *J. Mol. Struct.*, 2026, **1349**, 143904.
51 M. Abdel-Megid, M. E. Salem, M. A. Habib, M. R. Shaaban, I. A. Abdelhamid and A. H. M. Elwahy, *J. Mol. Struct.*, 2026, **1349**, 143700.
52 M. A. Ragheb, H. K. Abdelhakim, L. O. Mostafa, I. A. Abdelhamid, H. M. Hassaneen, E. M. Elzayat, F. M. Saleh and M. H. Soliman, *Process Biochem.*, 2026, **165**, 111–125.
53 R. E. Abdelwahab, M. E. Salem, M. R. Alsulami, A. H. M. Elwahy, K. Barakat, A. M. Abdelmoniem, N. Raza and I. A. Abdelhamid, *J. Mol. Struct.*, 2026, **1357**, 145165.
54 M. T. Helmy, H. M. Hassaneen, I. A. Abdelhamid, E. M. Zayed and Y. N. Laboud, *Tetrahedron*, 2026, **194**, 135183.
55 I. A. Abdelhamid, K. Barakat, F. G. Mohamed, M. A. Ragheb, H. M. Diab, A. M. Abdelmoniem and A. H. M. Elwahy, *J. Mol. Struct.*, 2026, **1357**, 145256.
56 N. S. Ibrahim, A. A. WalyEldeen, S. A. Ibrahim, I. A. Abdelhamid, H. K. A. Elhakim and N. Schmiedebergs, *Arch. Pharmacol.*, 2026, **399**, 8867–8882.
57 D. H. Ali, M. M. Soliman, H. M. Diab, T. A. Abdallah, M. E. Salem, I. A. Abdelhamid and A. H. M. Elwahy, *ChemistrySelect*, 2026, **11**, e06102.
58 N. S. Ibrahim, A. A. WalyEldeen, S. A. Ibrahim, I. A. Abdelhamid and H. K. A. Elhakim, *Naunyn-Schmiedeberg's Arch. Pharmacol.*, 2026, **2026**, 1–16.
59 A. Abdelgawad, M. E. Salem, S. M. A. Soliman, I. A. Abdelhamid, M. Abdel-Megid and A. M. Elgamal, *Macromol. Res.*, 2026, 1–14.
60 M. A. Ragheb, M. E. Salem, A. A. Hamed, I. A. Abdelhamid, H. A. Ali, M. Abdel-Megid and A. M. Elgamal, *Int. J. Biol. Macromol.*, 2025, **331**, 148298.
61 M. F. Mohamed, A. A. Hamed, A. A. Kashmiry, A. A. Saddiq, I. A. Abdelhamid and A. M. Elgamal, *Int. J. Biol. Macromol.*, 2025, **308**, 142048.
62 A. M. Elgamal, M. E. Salem, A. A. Hamed, I. A. Abdelhamid, T. A. Abdallah, H. A. Ali, N. Raza and M. A. Ragheb, *Carbohydr. Polym.*, 2025, **369**, 124258.
63 I. M. Z. Fares, M. E. Salem, M. S. Shafik, I. A. Abdelhamid, A. H. M. Elwahy, N. S. Ibrahim, M. Abdel-Megid and H. M. Diab, *J. Mol. Struct.*, 2025, **1339**, 142345.
64 A. A. Kashmiry, N. S. Ibrahim, M. F. Mohamed and I. A. Abdelhamid, *Polycyclic Aromat. Compd.*, 2025, **45**, 560–579.
65 M. E. Salem, A. F. Darweesh, A. M. Farag and A. H. M. Elwahy, *Tetrahedron*, 2016, **72**, 712–719.
66 H. M. Diab, A. M. Abdelmoniem, M. R. Shaaban, I. A. Abdelhamid and A. H. M. Elwahy, *RSC Adv.*, 2019, **9**, 16606–16682.
67 M. A. Ragheb, H. E. Abdelrashid, E. M. Elzayat, I. A. Abdelhamid and M. H. Soliman, *J. Biomol. Struct. Dyn.*, 2025, **43**, 9139–9157.
68 S. Abdel Halim and H. M. E. Hassaneen, *RSC Adv.*, 2022, **12**, 35794–35808.
69 N. A. Abd El-Fatah, A. F. Darweesh, A. A. Mohamed, I. A. Abdelhamid and A. H. M. Elwahy, *Tetrahedron*, 2017, **73**, 1436–1450.
70 H. M. Diab, M. E. Salem, A. H. M. Elwahy and I. A. Abdelhamid, *Synth. Commun.*, 2021, **51**, 2001–2015.
71 H. O. Huisman, *Angew Chem. Int. Ed. Engl.*, 1971, **10**, 450–459.
72 C. R. Engel and M. N. Roy Chowdhury, *Tetrahedron Lett.*, 1968, **9**, 2107–2111.
73 M. Gumulka, I. H. Ibrahim, Z. Boncza-Tomaszewski and C. R. Engel, *Can. J. Chem.*, 1985, **63**, 766–772.
74 C. R. Engel, D. Mukherjee, M. N. Roy Chowdhury, G. Ramani and V. S. Salvi, *J. Steroid Biochem.*, 1975, **6**, 585–597.
75 M. F. Mohamed, M. S. Mohamed, S. A. Shouman, M. M. Fathi and I. A. Abdelhamid, *Appl. Biochem. Biotechnol.*, 2012, **168**, 1153–1162.
76 A. T. L. Dos Santos, J. B. de Araújo-Neto, M. M. C. da Silva, M. E. P. da Silva, J. N. P. Carneiro, V. J. A. Fonseca, H. D. M. Coutinho, P. N. Bandeira, H. S. Dos Santos and F. R. da Silva Mendes, *Microb. Pathog.*, 2023, **180**, 106129.
77 P. Jeschke, *Pest Manage. Sci.*, 2010, **66**, 10–27.
78 M.-L. Hsieh and J. Borger, in *StatPearls*, StatPearls Publishing, 2023.
79 M. Balouiri, M. Sadiki and S. K. Ibnsouda, *J. Pharm. Anal.*, 2016, **6**, 71–79.
80 I. Chopra and M. Roberts, *Microbiol. Mol. Biol. Rev.*, 2001, **65**, 232–260.
81 E. A. Meyer, R. K. Castellano and F. Diederich, *Angew. Chem., Int. Ed.*, 2003, **42**, 1210–1250.
82 C. Bissantz, B. Kuhn and M. Stahl, *J. Med. Chem.*, 2010, **53**, 5061–5084.
83 R. O'Shea and H. E. Moser, *J. Med. Chem.*, 2008, **51**, 2871–2878.
84 L. J. V Piddock, *Nat. Rev. Microbiol.*, 2006, **4**, 629–636.
85 M. F. Mohamed, M. S. Mohamed, S. A. Shouman, M. M. Fathi and I. A. Abdelhamid, *Appl. Biochem. Biotechnol.*, 2012, **168**, 1153–1162.

86 A. A. Hamed, I. A. Abdelhamid, G. R. Saad, N. A. Elkady and M. Z. Elsabee, *Int. J. Biol. Macromol.*, 2020, **153**, 492–501.
87 C. H. Teh, W. A. Nazni, A. H. Nurulhusna, A. Norazah and H. L. Lee, *BMC Microbiol.*, 2017, **17**, 36.
88 M. Stupar, M. L. Grbić, A. Džamić, N. Unković, M. Ristić, A. Jelikić and J. Vukojević, *S. Afr. J. Bot.*, 2014, **93**, 118–124.
89 B. Baby, V. Ravisankar, L. S. Nair and P. A. Nazeem, *Int. J. Pharm. Sci. Res.*, 2016, **7**(3), 1125–1130.
90 G. M. Morris, R. Huey, W. Lindstrom, M. F. Sanner, R. K. Belew, D. S. Goodsell and A. J. Olson, *J. Comput. Chem.*, 2009, **30**, 2785–2791.
91 Y. Liu, X. Yang, J. Gan, S. Chen, Z.-X. Xiao and Y. Cao, *Nucleic Acids Res.*, 2022, **50**, W159–W164.
92 T. M. Fakih and M. L. Dewi, *J. Trop. Pharm. Chem.*, 2021, **5**, 347–352.
93 N. Salem, K. Msaada, S. Elkahoui, G. Mangano, S. Azaeiz, I. Ben Slimen, S. Kefi, G. Pintore, F. Limam and B. Marzouk, *BioMed Res. Int.*, 2014, **2014**, 762397.